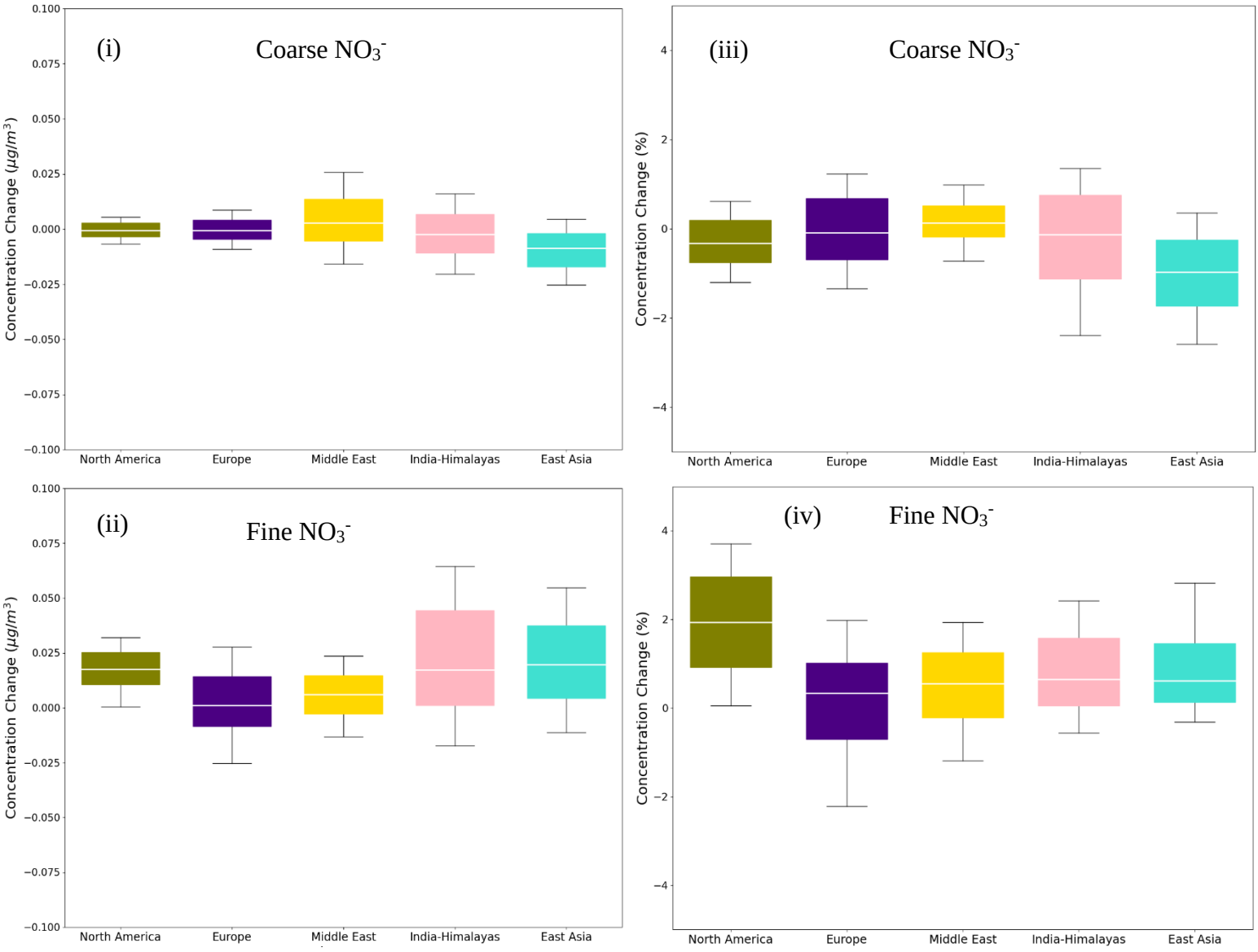

Figure S1: Bar chart plots depicting the 25th, 50th and 75th percentiles (box) of the difference in the global daily mean surface concentrations of i) coarse and ii) fine aerosol NO_3^- for the regions of North America, Europe, Middle East, India-Himalayas and East Asia, as predicted by EMAC using ISORROPIA II v1 and ISORROPIA II v2.3. The fractional differences in global daily mean surface concentrations of iii) coarse and iv) fine aerosol NO_3^- for the same regions are also shown. Both models assume that the aerosol is at its stable state at low RH and a positive change corresponds to higher concentrations by ISORROPIA II v1.

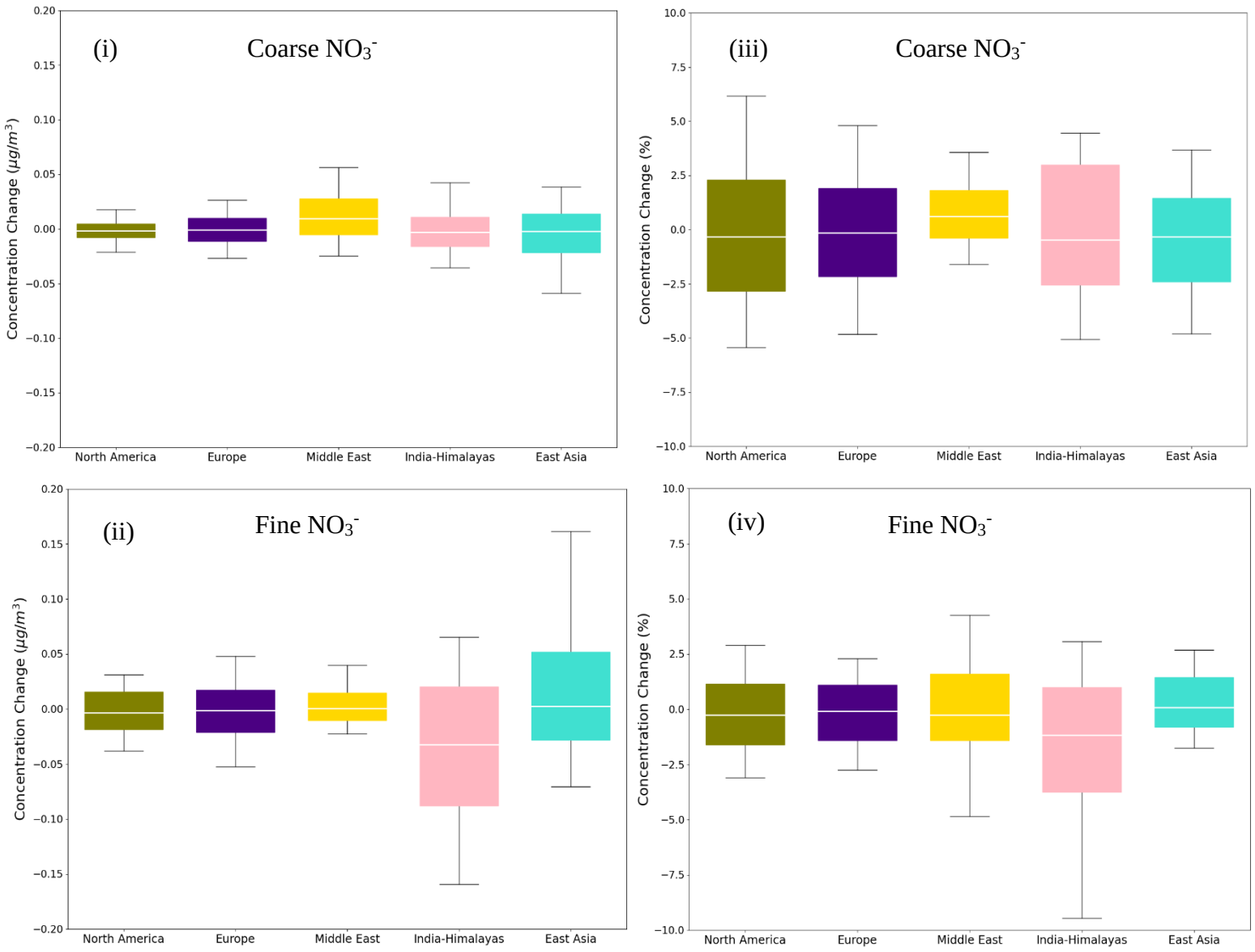

Figure S2: Bar chart plots depicting the 25th, 50th and 75th percentiles (box) of the difference in the global daily mean surface concentrations of i) coarse and ii) fine aerosol NO_3^- for the regions of North America, Europe, Middle East, India-Himalayas and East Asia, as predicted by EMAC using ISORROPIA-lite and ISORROPIA II. The fractional differences in global daily mean surface concentrations of iii) coarse and iv) fine aerosol NO_3^- for the same regions are also shown. Both models assume that the aerosol is at its metastable state at low RH and a positive change corresponds to higher concentrations by ISORROPIA-lite.

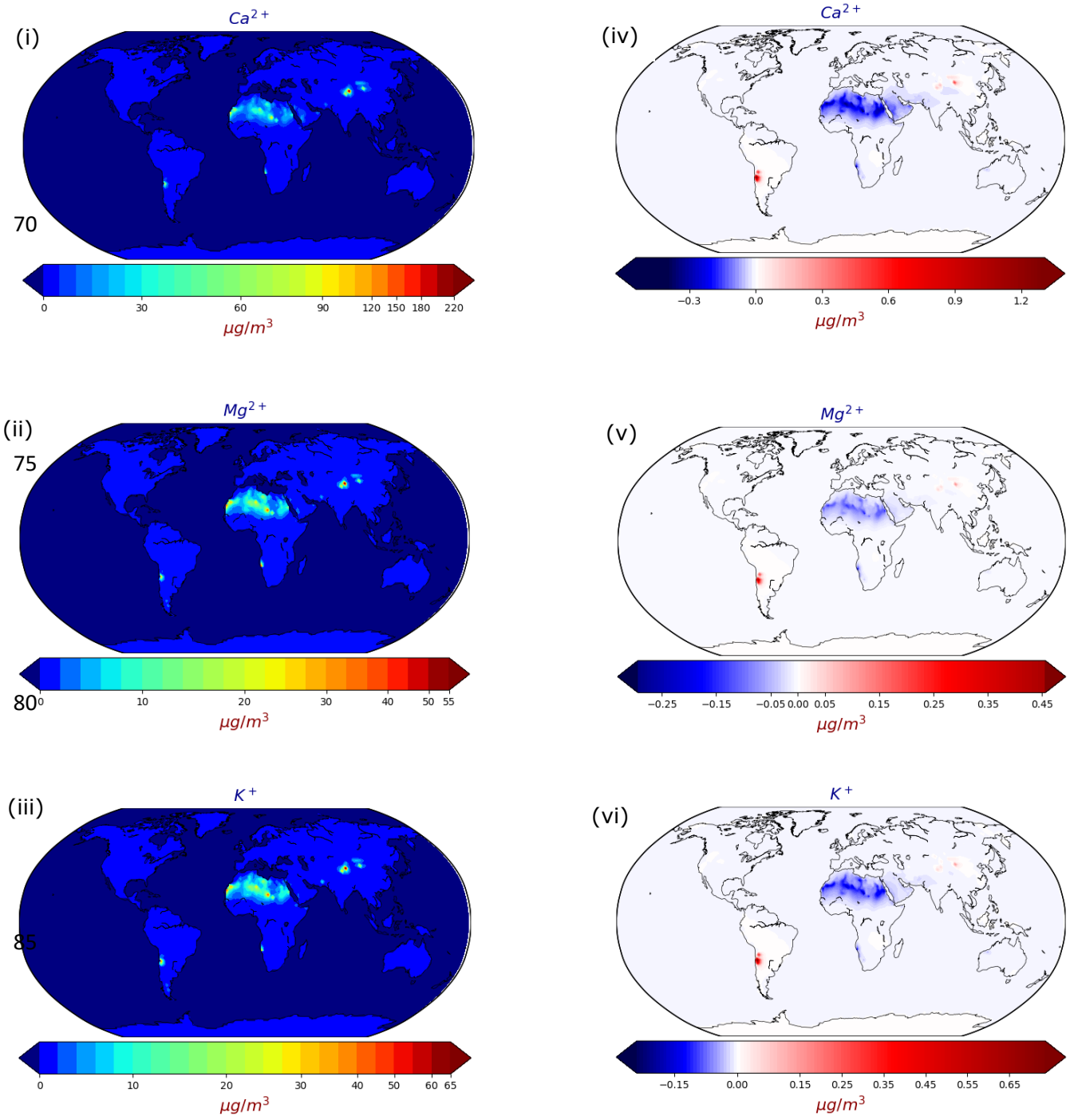

Figure S3: Annual mean surface concentrations of i) Ca^{2+}, ii) Mg^{2+} and iii) K^+ in TSP as predicted by EMAC using ISORROPIA-lite. Change of the annual mean EMAC-simulated surface concentration of iv) Ca^{2+}, v) Mg^{2+} and vi) K^+ in TSP after employing ISORROPIA II. Positive values in red indicate higher concentrations by ISORROPIA-lite. The models assume different aerosol states.